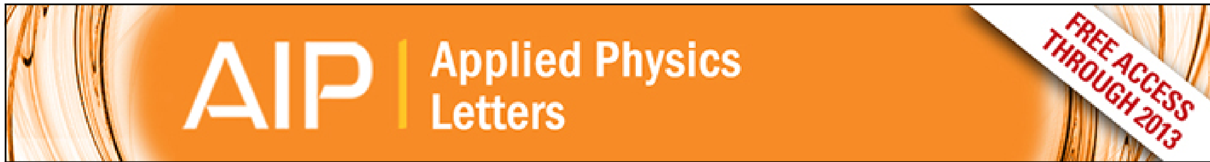

Structural study of refractory-metal-free C40 TiSi 2 and its transformation to C54 TiSi 2

T. Yu, S. C. Tan, Z. X. Shen, L. W. Chen, J. Y. Lin, and A. K. See

Citation: Applied Physics Letters **80**, 2266 (2002); doi: 10.1063/1.1466521
View online: http://dx.doi.org/10.1063/1.1466521
View Table of Contents: http://scitation.aip.org/content/aip/journal/apl/80/13?ver=pdfcov
Published by the AIP Publishing

Re-register for Table of Content Alerts

Create a profile.
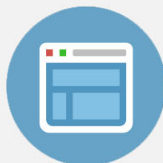
Sign up today!

This article is copyrighted as indicated in the article. Reuse of AIP content is subject to the terms at: http://scitation.aip.org/termsconditions. Downloaded to IP: 155.69.4.4 On: Wed, 11 Dec 2013 04:45:52

Structural study of refractory-metal-free C40 $TiSi_2$ and its transformation to C54 $TiSi_2$

T. Yu,[a] S. C. Tan, Z. X. Shen, L. W. Chen, and J. Y. Lin
Physics Department, 2 Science Drive 3, Faculty of Science, National University of Singapore, Singapore 117542

A. K. See
Chartered Semiconductor Manufacturing Limited, 60 Woodlands Industrial Park D, Street 2, Singapore 738406, Republic of Singapore

(Received 13 November 2001; accepted for publication 1 February 2002)

The structure of laser-induced refractory-metal-free C40 $TiSi_2$ has been studied by glancing-angle x-ray diffraction (GAXRD) in detail. The result shows that laser-induced C40 $TiSi_2$ has a hexagonal structure with the $P6_222$ space group and lattice parameters $a=0.467$ nm and $c=0.662$ nm. The ordering effect and the stress effect on the $TiSi_2$ film are also discussed based on the GAXRD and micro-Raman results. The C40 phase completely transforms to the technologically important C54 phase at a relatively low temperature of 700 °C. © *2002 American Institute of Physics.*
[DOI: 10.1063/1.1466521]

The formation of C54 $TiSi_2$ has attracted a great deal of attention owing to its significant technological importance in the self-aligned silicide (salicide) processes in ultra-large-scale integration. In a typical salicide process in semiconductor device fabrication, a layer of silicide thin film is formed by reaction between the deposited metal Ti and Si surfaces on gate, source, and drain areas during rapid thermal processing (RTP). As is well known, C49 $TiSi_2$, a metastable phase of $TiSi_2$ with a high resistivity of 60–90 $\mu\Omega$ m was usually observed before the formation of C54 $TiSi_2$, which has low resistivity ($\sim$15 $\mu\Omega$ m) and high thermal stability.[1–5] However, this C49–C54 $TiSi_2$ phase transformation becomes very difficult and incomplete for subquarter micron devices due to the lack of sufficient C49 $TiSi_2$ triple-grain boundaries where C54 $TiSi_2$ nucleate.[5,6]

Recently, significant breakthroughs were reported in which the C54 phase was epitaxally formed from a metastable C40 phase bypassing the C49 phase. Mann *et al.*,[7] and Kittl, Gribelyuk, and Samavedam[8] observed that the C40 phase acts as a template allowing the direct formation of the C54 phase and blocking the formation of the C49 phase when a small amount of Mo ions were implanted into the Si substrate prior to Ti film deposition. Another method of forming C40 $TiSi_2$ is by depositing a thin Mo layer of 1 nm in thickness between the Ti film and Si substrate as demonstrated by Mouroux *et al.*[9] However, as Chen *et al.*[10] discussed, the use of refractory metals also raised several important issues. More recently, the refractory-metal-free C40 $TiSi_2$ was synthesized by Chen *et al.*,[10] using a laser-annealing process and identified by Li, Chen, and Shen[11] using convergent beam electron diffraction (CBED) and CBED pattern simulation. In their work, the formation of C40 $TiSi_2$ was attributed to kinetic factors resulting from the extreme thermal nonequilibrium induced by the pulsed laser annealing.

As a new $TiSi_2$ phase, the crystal structure of C40 $TiSi_2$ has been systematically investigated by high-resolution transmission electron microscopy (HRTEM),[11] and the direct phase transformation from the C40 phase to C54 phase was studied by Raman spectroscopy.[10,11] However, the pure C40–C54 transformation bypassing the C49 $TiSi_2$ phase has never been studied by x-ray diffraction (XRD), even the XRD pattern of the pure C40 phase resulting from the refractor-metal-free Ti/Si samples. In this work, we used x-ray diffraction to characterize C40 $TiSi_2$ directly formed by pulsed laser annealing a pure Ti/Si sample and the C40–C54 $TiSi_2$ phase transformation upon further RTP annealing.

The preparation of precursor Ti/Si samples and the pulsed laser annealing process has been reported in detail by Chen *et al.*[10] and Li, Chen, and Shen.[11] A Digital Instruments (Dimension™ 3000 SPM) atomic-force microscope (AFM) with tapping mode was used to demonstrate the morphology and average grain size of pure C40 $TiSi_2$ induced by laser annealing. A RTP processor (Jipelec JetFirst system) was employed to transform pure C40 $TiSi_2$ to C54 $TiSi_2$ by heating the samples at different temperatures for 60 s. The samples after various temperature RTP treatments were identified by a SPEX 1702/04 micro-Raman spectrometer with a He–Ne laser ($\lambda=632.8$ nm) as the excitation source.

Figure 1(a) shows the typical top-view AFM image of the laser-irradiated sample after etching in $NH_4OH:H_2O_2:H_2O=1:1:6$ for complete removal of the unreacted surface Ti film. As shown, the average grain size is about 50 nm with a high uniformity of grain size and distribution.

Figure 1(b) (bottom spectrum) displays the Raman modes of the same as-laser-annealed sample. Compared with the previous results,[10,11] it is obvious that pure C40 $TiSi_2$ is the dominant phase after the laser annealing process in this work.

The crystal structure of C40 $TiSi_2$ has been identified using HRTEM by Li, Chen, and Shen[11] and normal Bragg–Bentano XRD by Via *et al.*[12] By using glancing-angle XRD

[a]Author to whom correspondence should be addressed; electronic mail: scip9600@nus.edu.sg

This article is copyrighted as indicated in the article. Reuse of AIP content is subject to the terms at: http://scitation.aip.org/termsconditions. Downloaded to IP: 155.69.4.4 On: Wed, 11 Dec 2013 04:45:52

 © 2002 American Institute of Physics

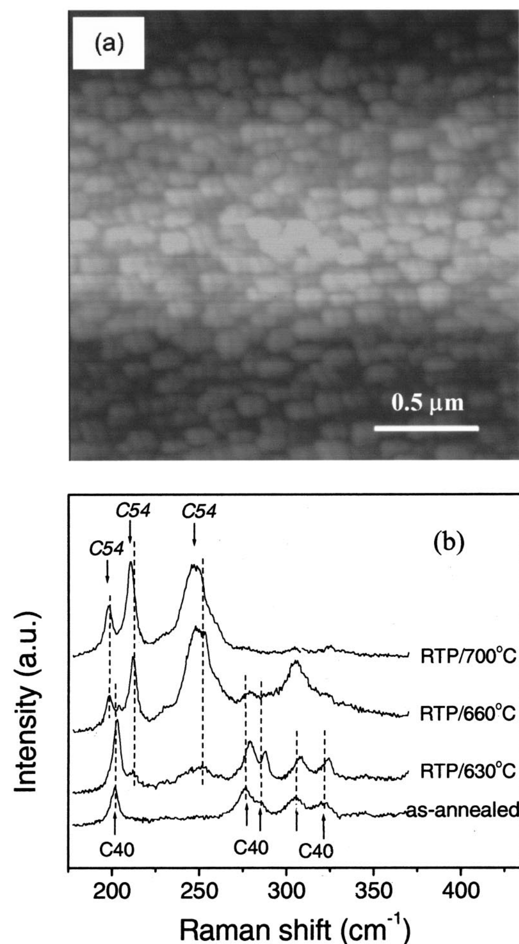

FIG. 1. (a) AFM image of the $TiSi_2$ C40 phase produced by laser anneal of the Ti/Si sample. (b) Raman spectra of the C40 phase before and after RTP treatments.

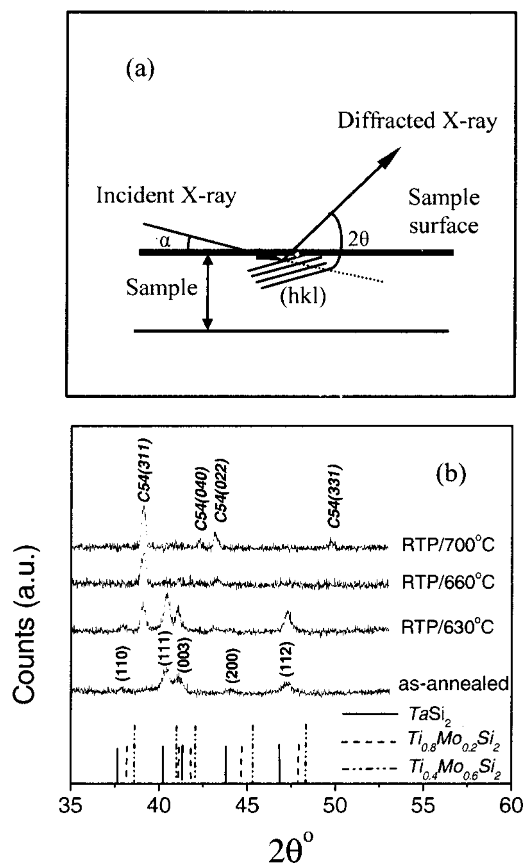

FIG. 2. (a) Schematic diagram of the GAXRD geometry, incidence angle α of the x ray is fixed at 2° and the detector is scanned during experiment. (b) XRD patterns of the as-laser-annealed C40 $TiSi_2$ sample before and after RTP treatments.

(GAXRD) operating under the detector scan mode to analyze the samples instead of the common Bragg–Bentano XRD (BBXRD) method, which operates at the θ–2θ mode, we can effectively multiply the x-ray diffraction by the surface $TiSi_2$ thin film and strongly reduce the penetration depth and collection time.[13] The crystal structure of the refractory-metal-free C40 $TiSi_2$ and C40–C54 phase transformations were studied by GAXRD at room temperature. In this work, XRD patterns were taken using a D8 ADVANCE x-ray diffractometer (Bruker Analytical X-Ray Systems). A Cu $K\alpha_1$ x-ray source ($\lambda = 1.5406$ Å) was used at 40 kV and 40 mA. The GAXRD diffraction geometry is shown schematically in Fig. 2(a). The incidence angle α was fixed at 2° relative to the sample surface while the detector was rotated to collect the diffracted x-ray during the scan. As shown in Fig. 2(b) (bottom curve), the GAXRD pattern of pure C40 $TiSi_2$ presents five peaks at 37.96°, 40.43°, 41.04°, 43.92°, and 47.24°. For comparison, the XRD peak positions for the $Ti_{0.4}Mo_{0.6}Si_2$ (Ref. 14a) ($a = 0.465$ nm, $c = 0.650$ nm), $Ti_{0.8}Mo_{0.2}Si_2$ (Ref. 14b) ($a = 0.470$ nm, $c = 0.652$ nm), and $TaSi_2$ (Ref. 14c) ($a = 0.478$ nm, $c = 0.657$ nm) were also indicated in Fig. 2(b). It is obvious that the XRD peaks of laser-induced refractory-metal-free C40 $TiSi_2$ match well with the other well-known C40 phase silicides, all of which have the hexagonal crystal structure with space group $P6_222$ (180). Especially, the peak positions of laser-induced C40 $TiSi_2$ are quite close to that of $TaSi_2$. This can be explained as the small difference in lattice parameters between C40 $TiSi_2$ and $TaSi_2$ as reported by Via *et al.*[12] It is noted that the results of Li, Chen, and Shen[11] have shown that pure C40 $TiSi_2$ has a hexagonal structure ($P6_222$). Therefore, we set the XRD pattern shown in Fig. 2(b) (bottom) as the hexagonal structure with space group $P6_222$. After addressing the five peaks to the (110), (111), (003), (200), and (112) planes of C40 $TiSi_2$, we obtained the experimental lattice parameters ($a = 0.467$ nm, $c = 0.662$ nm) of pure C40 $TiSi_2$. It is well matched with the HRTEM results ($a = 0.471$ nm, $c = 0.653$ nm),[11] and BBXRD results ($a = 0.469$ nm, $c = 0.649$ nm).[12] Our experimental results for the interplanar distance, 2.19 Å for the (003) plane, 2.23 Å for the (111) plane, and 1.92 Å for the (112) plane, also show excellent agreement with the HRTEM results of 2.18, 2.21, and 1.92 Å, respectively.[11]

In order to study the phase transformation from C40 $TiSi_2$ to C54 $TiSi_2$, we used RTP to anneal the laser-induced C40 $TiSi_2$ sample at various temperatures for the same duration (60 s). Figure 2(b) illustrates the GAXRD patterns of C40 $TiSi_2$ after annealing at different temperatures. As shown, the C54 phase appears after a relative low-temperature ($T = 630$ °C) RTP treatment. Interestingly, the peak intensity of XRD peaks belonging to C40 $TiSi_2$ increases dramatically with a large reduction of the full width at half maximum (FWHM), even after the appearance of the C54 phase. By considering the typical x-ray diffraction theory, it is quite reasonable to attribute this phenomenon to

This article is copyrighted as indicated in the article. Reuse of AIP content is subject to the terms at: http://scitation.aip.org/termsconditions. Downloaded to IP: 155.69.4.4 On: Wed, 11 Dec 2013 04:45:52

the ordering and perfecting process of crystalline C40 $TiSi_2$ caused by low-temperature RTP annealing. Notice that the coexistence of the more-ordered C40 phase, and the C54 phase is strongly related to the epitaxial growth behavior between C40 $TiSi_2$ and C54 $TiSi_2$. With the increase in temperature, the dominant phase transforms from the C40 $TiSi_2$ before RTP to the C54 $TiSi_2$ after RTP at 660 °C for 60 s. Further annealing (T=700 °C) completely transforms C40 $TiSi_2$ to C54 $TiSi_2$, characterized by the XRD pattern of the pure C54 $TiSi_2$ phase.[15] Our XRD results indicate that C49 $TiSi_2$ is never formed for all RTP treated (T=625–700 °C) laser-induced C40 $TiSi_2$ samples. Hence, the laser-induced refractory-metal-free C40 $TiSi_2$ can greatly decrease the C54 $TiSi_2$ formation temperature and directly transform to the C54 phase, completely bypassing the C49 $TiSi_2$.

Figure 1(b) also shows the Raman spectra of the samples corresponding to the GAXRD patterns shown in Fig. 2(b), which strongly support the conclusions drawn from the XRD study that the laser-induced refractory-metal-free C40 $TiSi_2$ can directly transform to C54 $TiSi_2$, bypassing the C49 phase. A detailed Raman study has been presented by Chen *et al.*[10] that demonstrated the same result. Similar to the XRD peaks, the Raman peaks of the C40 phase also display a dramatic increase of intensity and decrease of FWHM. Peak splitting at around 280 cm^{-1} is clearly seen in the 630 °C annealed spectrum, corresponding to a more-ordered C40 $TiSi_2$ phase. More interestingly, an obvious blueshift of the C40 $TiSi_2$ vibrational modes occurs with increasing RTP temperature while a slight redshift of the C54 $TiSi_2$ vibrational modes can be observed with further annealing. The Raman mode shifts most likely result from stress, which is mainly caused by the mismatch between the substrate Si and the C40 $TiSi_2$ as well as between C40 and C54 $TiSi_2$. Raman modes are very sensitive to stress, and different kinds of stress (compress or tensile) induce contrast shifts (blueshift or redshift)[16] in the Raman spectra.

In conclusion, the structure of laser-induced refractory-metal-free C40 $TiSi_2$ has been studied using GAXRD. Both GAXRD and the Raman study unambiguously demonstrate that this laser-induced C40 $TiSi_2$ can directly transform to C54 $TiSi_2$, bypassing C49 $TiSi_2$ at a relatively low temperature.

[1] K. Maex, Mater. Sci. Eng., R. **11**, 53 (1993).
[2] J. A. Kittl, D. A. Prinslow, P. P. Apte, and M. F. Pas, Appl. Phys. Lett. **67**, 2308 (1995).
[3] J. B. Lasky, J. S. Nakos, O. J. Cain, and P. J. Geiss, IEEE Trans. Electron Devices **ED-38**, 262 (1991).
[4] M. H. Wang and L. J. Chen, J. Appl. Phys. **71**, 5918 (1992).
[5] Z. Ma, L. H. Allen, and D. D. Allman, J. Appl. Phys. **77**, 4384 (1995).
[6] Z. Ma and L. H. Allen, Phys. Rev. B **49**, 13501 (1994).
[7] R. W. Mann, G. L. Miles, T. A. Knotts, D. W. Rakowski, L. A. Clevenger, J. M. E. Harper, F. M. d'Heurle, and C. Cabra, Jr., Appl. Phys. Lett. **67**, 3729 (1995).
[8] J. A. Kittl, M. A. Gribelyuk, and S. B. Samavedam, Appl. Phys. Lett. **73**, 900 (1998).
[9] A. Mouroux, S.-L. Zhang, W. Kaplan, S. Nygren, M. Östling, and C. S. Petersson, Appl. Phys. Lett. **69**, 975 (1996).
[10] S. Y. Chen, Z. X. Shen, K. Li, A. K. See, and L H. Chan, Appl. Phys. Lett. **77**, 4395 (2000).
[11] K. Li, S. Y. Chen, and Z. X. Shen, Appl. Phys. Lett. **78**, 3989 (2001).
[12] F. La. Via, F. Mammoliti, G. Corallo, M. G. Grimaldi, D. B. Migas, and L. Miglio, Appl. Phys. Lett. **78**, 1864 (2001).
[13] P. N. Gibson, M. E. Özsan, D. Lincot, P. Cowache, and D. Summa, Thin Solid Films **361-362**, 34 (2000).
[14] (a) JCPDS-International Centre for diffracton Data No. 06-0607; (b) Data No. 07-0331; (c) Data No. 38-0483.
[15] J. A. Kittl, Q. Z. Hong, H. Yang, N. Yu, S. B. Samvedam, and M. A. Gribelyuk, Thin Solid Films **332**, 404 (1998).
[16] M. S. Chen, Z. X. Shen, S. H. Tan, W. S. Shi, D. F. Cui, and Z. H. Chen, J. Phys.: Condens. Matter **12**, 1 (2000).

This article is copyrighted as indicated in the article. Reuse of AIP content is subject to the terms at: http://scitation.aip.org/termsconditions. Downloaded to IP: 155.69.4.4 On: Wed, 11 Dec 2013 04:45:52